ADVANCES IN ATMOSPHERIC SCIENCES, VOL. 23, NO. 5, 2006, 750–757

On the Nonlinear Response of Lower Stratospheric Ozone to NO_x and ClO_x Perturbations for Different CH_4 Sources

WANG Geli* (王革丽) and YANG Peicai (杨培才)

Institute of Atmospheric Physics, Chinese Academy of Sciences, Beijing 100029

(Received 12 December 2005; revised 13 February 2006)

ABSTRACT

The impact of sulfate aerosol, ClO_x and NO_x perturbations for two different magnitudes of CH_4 sources on lower stratospheric ozone is studied by using a heterogeneous chemical system that consists of 19 species belonging to 5 chemical families (oxygen, hydrogen, nitrogen, chlorine and carbon). The results show that the present modeled photochemical system can present several different solutions, for instance, periodic states and multi-equilibrium states appearing in turn under certain parameter domains, through chlorine chemistry and nitrogen chemistry together with sulfate aerosol as well as the increasing magnitude of CH_4 sources. The existence of catastrophic transitions could produce a dramatic reduction in the ozone concentration with the increase of external sources.

Key words: lower stratosphere, atmospheric ozone, aerosol, multi-equilibrium, catastrophic transition

doi: 10.1007/s00376-006-0750-6

1. Introduction

The extensive experimental and modeling studies of the last decade provide much evidence for the key role of photochemical processes in the observed ozone loss in the stratosphere, and this effect determines the particular importance of the investigations of photochemistry for this region.

In recent years, both the measurement in laboratories and model analyses have revealed that the heterogeneous reactions happening on the surface of aerosol are important and could lead to depletion of ozone (Worsnop et al., 1988; Mozurkewich and Calvert, 1988; Hofmann and Solomon, 1989; Rodriguez et al., 1991; Granier and Brasseur, 1992; WMO, 1992; Fried et al., 1994; Tie et al., 1994; Bojkov, 1995). In a general way, the total surface area of aerosols participating in heterogeneous reactions in a unit volume is low, since the sizes of aerosols are very small in the lower stratosphere. Usually, it is just of the magnitude of 10^{-8} $cm^2\,cm^{-3}$, which corresponds to the aerosol concentration before 1970 and referrs to the background or current value. However, because several intensive volcanic eruptions have happened in recent years, for example, the Elchichou event in 1982 and the Pinatubo event in 1991, a lot of matter with sulphide was projected into the stratosphere, and this was able to lead to the increase of aerosol concentration there. The observations show that the aerosol concentrations reached a value of about $(10–100)\times10^{-8}$ cm^{-1} after the Pinatubo eruption (Hofmann and Solomon, 1989; Prather, 1992; McCormick and Veiga, 1992). Under these aerosol conditions, the influence of aerosol perturbation on ozone in the stratosphere has received more and more attention.

In addition, models of various atmospheric photochemical systems have been analyzed by Prather et al. (1979), White and Dietz (1984), Kasting and Ackerman (1985), Stewart (1993,1995), Yang and Brasseur (1994, 2001) and Konovalov et al. (1999). Their studies have revealed that under certain circumstances atmospheric chemical systems could exhibit multiple equilibrium solutions which produce catastrophic transitions. This research focusing on the nonlinear behavior of the atmospheric chemical system has suggested that the photochemical processes are complex and have the possibility to exhibit unexpected serious consequences in response to external forcing like some anthropogenic and natural perturbations.

Globally, fossil fuel combustion and natural sources are major sources of hydrocarbons (mostly CH_4) which cause CH_4 concentrations to increase in the atmosphere (WMO, 1995). Methane (CH_4) is the most abundant hydrocarbon in the atmosphere and is useful as a tracer of atmospheric circulation because of its long photochemical lifetime (8–9 years in the global atmosphere), also it can not be created directly by chemical or photolytic reactions in the stratosphere.

*E-mail: wgl@mail.iap.ac.cn

Under these considerations, an important motivation for our work has been the desire to analyze the behavior of the lower stratospheric photochemical system in response to enhanced atmospheric abundances of sulfate aerosol and reactive nitrogen and chlorine along with increasing CH_4 sources. This is an extended research based on the former studies by Yang and Brasseur (2001, 2004).

Below we present our results in the following order. In section 2, we briefly describe the model used in the present study; in section 3, we evaluate the response of the photochemical system to external forcing strengthened by nitrogen with the aerosol surface area density for two different magnitudes of CH_4 sources; and in section 4, we assess the response of the photochemical system to chlorine together with the aerosol surface area density for two different CH_4 sources.

2. Model

The model used in this study is a zero-dimensional box model, in which the adopted chemical scheme is similar to that used by Yang and Brasseur (2004), except it is applied at 18 km altitude which enables it to exhibit the average circumstance of the low stratospheric atmosphere.

Table 1. Chemical reactions included in this heterogeneous model and their rates.

	Reaction	Reaction rate* (cm^3 s^{-1})
1	$O+O_2+M \rightarrow O_3+M$	1.0×10^{-15}
2	$O+O_3 \rightarrow 2O_2$	6.03×10^{-16}
3a	$O(^1D)+N_2 \rightarrow O+N_2$	2.98×10^{-11}
3b	$O(^1D)+O_2 \rightarrow O+O_2$	4.42×10^{-11}
4	$H_2O+O(^1D) \rightarrow 2OH$	2.2×10^{-10}
5	$OH+O_3 \rightarrow O_2+HO_2$	2.1×10^{-14}
6	$HO_2+O_3 \rightarrow 2O_2+OH$	1.09×10^{-15}
7	$HO_2+HO_2 \rightarrow H_2O_2+O_2$	3.65×10^{-12}
8	$OH+H_2O_2 \rightarrow H_2O+HO_2$	1.39×10^{-12}
9	$OH+HO2 \rightarrow H_2O+O_2$	1.52×10^{-10}
10	$HO_2+O \rightarrow O_2+OH$	7.54×10^{-11}
11	$NO+O_3 \rightarrow NO_2+O_2$	3.16×10^{-15}
12	$NO_2+O \rightarrow NO+O_2$	1.13×10^{-11}
13	$NO_2+O_3 \rightarrow NO_3+O_2$	1.5×10^{-18}
14	$NO_2+NO_3+M \rightarrow N_2O_5+M$	1.6×10^{-12}
15	$N_2O_5+M \rightarrow NO_2+NO_3+M$	6.85×10^{-8}
16	$NO_2+OH+M \rightarrow HNO_3+M$	8.4×10^{-12}
17	$HNO_3+OH \rightarrow NO_3+H_2O$	3.67×10^{-13}
18	$NO+HO_2 \rightarrow NO_2+OH$	1.11×10^{-11}
19	$Cl+O3 \rightarrow ClO+O_2$	8.75×10^{-12}
20	$ClO+O \rightarrow Cl+O_2$	4.14×10^{-11}
21	$Cl+HO_2 \rightarrow O_2+HCl$	3.94×10^{-11}
22	$Cl+CH_4 \rightarrow HCl+CO+HO_2+H_2O$	1.74×10^{-14}
23	$ClO+NO \rightarrow Cl+NO_2$	2.44×10^{-11}
24	$ClO+NO_2+M \rightarrow ClONO_2+M$	1.33×10^{-12}
25	$ClO+HO_2 \rightarrow HOCl+O_2$	1.2×10^{-11}
26	$HCl+OH \rightarrow H_2O+Cl$	5.2×10^{-13}
27	$HOCl+OH \rightarrow H_2O+ClO$	2.99×10^{-13}
28	$OH+CH_4 \rightarrow 2H_2O+CO+HO_2$	6.87×10^{-16}
29	$O(^1D)+CH_4 \rightarrow CO+2H_2O$	1.5×10^{-10}
30	$CO+OH \rightarrow HO_2+CO_2$	1.5×10^{-13}
31	$ClO+ClO \rightarrow Cl_2O_2$	1.41×10^{-13}

* For three-body reactions, equivalent second-order rate constants are calculated for an air density of 2.72×10^{18} cm^{-3} at 18 km.

Table 2. Photolysis reactions used in the heterogeneous model.

	Reaction	J_k^* (s^{-1})
1	$O_2 + h\nu \rightarrow O+O$	4.0×10^{-14}
2	$O_3 + h\nu \rightarrow O_2+O(^1D)$	2.5×10^{-5}
3	$O_3 + h\nu \rightarrow O_2+O$	5.2×10^{-4}
4	$H_2O_2 + h\nu \rightarrow 2OH$	9.2×10^{-6}
5a	$NO_3 + h\nu \rightarrow NO_2+O$	1.56×10^{-1}
5b	$NO_3 + h\nu \rightarrow NO+O_2$	2.01×10^{-2}
6	$NO_2 + h\nu \rightarrow NO+O$	1.2×10^{-2}
7	$N_2O_5 + h\nu \rightarrow NO_2+NO_3$	2.3×10^{-5}
8	$HNO_3 + h\nu \rightarrow OH+NO_2$	6.0×10^{-7}
9a	$ClONO_2 + h\nu \rightarrow NO_3+Cl$	5.13×10^{-5}
9b	$ClONO_2 + h\nu \rightarrow NO_2+ClO$	5.7×10^{-6}
10	$HOCl+h\nu \rightarrow OH+Cl$	3.9×10^{-4}
11	$Cl_2O_2 + h\nu \rightarrow 2Cl+O_2$	2.30×10^{-3}

*Daytime values on 15 March at 40°N.

Similar to Yang and Brasseur (2004), the present model consists of 19 chemical species from the oxygen, hydrogen, nitrogen, chlorine, and carbon groups, which are determined by 45 homogeneous chemical and photochemical reactions and two heterogeneous reactions in sulfate aerosol; the chemical reactions and photolytic reactions are listed in Table 1 and Table 2 for 18 km altitude. Moreover, the atmospheric constituents for O_2 and H_2O are assumed to be stable, taken as 4.93×10^{17} cm^{-3} and 8.22×10^{12} cm^{-3}, respectively, at 18 km altitude. According to Yang and Brasseur (2001, 2004), the photolysis frequencies follow the same distribution with time. All the photochemical states are averages between the daytime and nighttime solutions, and all the photolysis rates represent the equinoctial condition at 40°N. Similar to Yang and Brasseur (2001, 2004), the solution of the numerically "stiff" nonlinear first-order differential equations is obtained by using the Gear algorithm (Gear, 1969).

Although it is relatively simple, the present model can capture the most important chemical processes that influence stratospheric ozone and can better describe the average characteristics of atmospheric components in the lower stratosphere.

The external sources of reactive nitrogen and chlorine (denoted as S_N and S_{Cl}) are assumed to arise from human activities such as the photo-oxidation of nitrous oxide (N_2O), the photolysis of chlorofluorocarbons (CFCs) and the in situ injection of NO_x from high altitude aircraft in the atmosphere. The compensating loss of nitrogen and chlorine due to the wet scavenging of nitric acid (HNO_3) and hydrogen chloride (HCl) is represented by the first order loss rates given in Table 3, and the loss rate for carbon monoxide (CO) and the current source strengths of reactive nitrogen and chlorine (S_N and S_{Cl}) are also given in the Table. The source (upward transport from the troposphere) of methane (S_{CH_4}) is assumed to be 1000 cm^{-3} s^{-1} (denoted as test-I) and 1800 cm^{-3} s^{-1} (denoted as test-II) for sensitivity analysis. In the following calculation, S_N and S_{Cl} together with aerosol surface area density A will be referred to as control parameters in this heterogenous photochemical model, where the nonlinear responses of the lower stratospheric ozone will be studied for different magnitude sources of CH_4 according to sensitivity test-I and test-II.

3. Response to the aerosol surface area density A and S_N

In order to simplify our analysis and focus on the impact of reactive nitrogen together with the aerosol surface area density A, the behavior of the chemical system is studied for A and different values of S_N chosen in the interval [115, 3000], S_{Cl} remains at the current value of 13, and other parameters are taken as the current values given in Tables 1, 2, 3 if not otherwise stated. This is equivalent to discussing the behaviors of the system in two dimensional parameter space of P (S_N, A).

3.1 *Result of test-I*

Figure 1 gives the solutions of the system when $115 \leqslant S_N \leqslant 3000$ and A are fixed at 1, 10, 100 and 150 for S_{CH_4} being 1000 cm^{-3} s^{-1}. It shows that solutions of this photochemical system include two branches of equilibrium states and multi-equilibrium solutions exist for certain parameters. In the case of $A = 1$ (Fig. 1a), the first equilibrium branch (in which the current

Table 3. Parameter values used in the heterogeneous model.

Parameter	Current value
1. first-order loss rate constants for HNO_3	1×10^{-8} s^{-1}
2. first-order loss rate constants for HCl	3×10^{-8} s^{-1}
3. first-order loss rate constants for CO	1×10^{-8} s^{-1}
4. source strength of ClO_x	13 cm^{-3} s^{-1}
5. source strength of NO_x	115 cm^{-3} s^{-1}

state is denoted by a dot) is denoted as the interval [115, 1620], and the second branch [1160, 3000]; the [1160, 1620] domain is characterized by multi-equilibrium solutions, while the two endpoints are the critical values leading to catastrophic transitions from one branch of solutions. When S_N is greater than 1620, increasing from the current value (equivalent to a 13-fold increase from the current value), the state of the system will jump from one stable equilibrium state to another, which will lead to an abrupt reduction in the ozone concentration by about 100 times and dramatic changes in the concentration of other chemical compounds. For A=10, from Fig. 1b, the corresponding multi-equilibrium period is [1835, 2580], and the topological structure of this system is not obviously different from Fig. 1a; however the width of its multi-equilibrium solutions increases by about 1.6 times, also its location is far away from the current value of S_N. For A=100, from Fig. 1c, the parameter interval of the multi-equilibrium solutions is near [1250, 2780], its width is more obviously increased and the location is much further away from the current value. If the parameter A is continually increased, for example, to reach A=150 (Fig. 1d), the location leads to a catastrophe transition that shows little change compared with A=100, and its topological structure in the state-parameter space also shows little change there. From Fig. 1, it shows that whatever the parameter S_N is, the system always keeps a "fold" catastrophe in the space $P(S_N, A)$. In addition, even when $A > 100$, the influence of A on the concentration caused by the catastrophe transition seems to be a little change for all species, and the topological structure of the system in the state-parameter space has no obvious change.

3.2 *Result of test-II*

In the comparison for S_{CH_4} equal to 1800 $cm^{-3}\ s^{-1}$ in this test, Fig. 2 gives the solutions of the system when the other parameters are given as in section 3.1. It is easy to see that the multi-equilibrium solutions

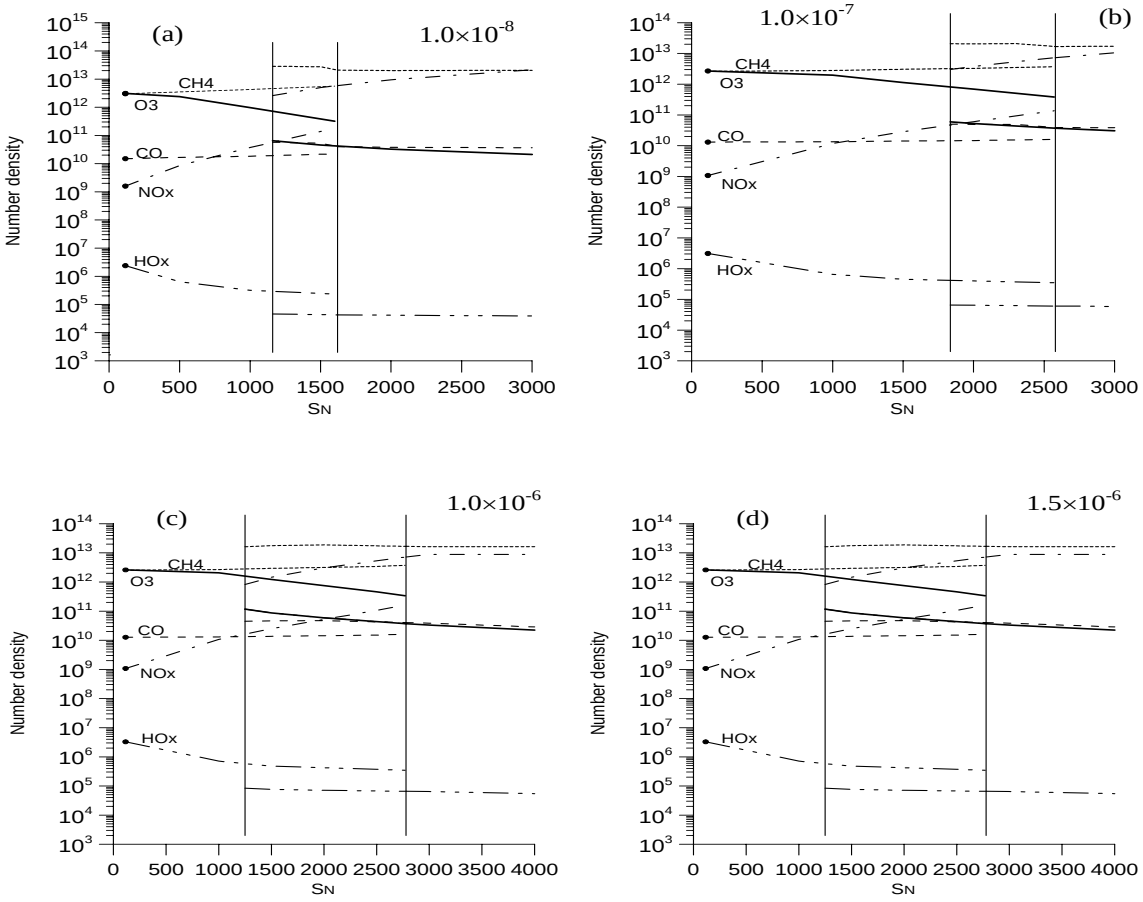

Fig. 1. Dependence of the states of the heterogeneous system on the aerosol surface area density A and the reactive nitrogen resource S_N for the source of CH_4 S_{CH_4} chosen as 1000 $cm^{-3}\ s^{-1}$ (units: cm^{-3}).

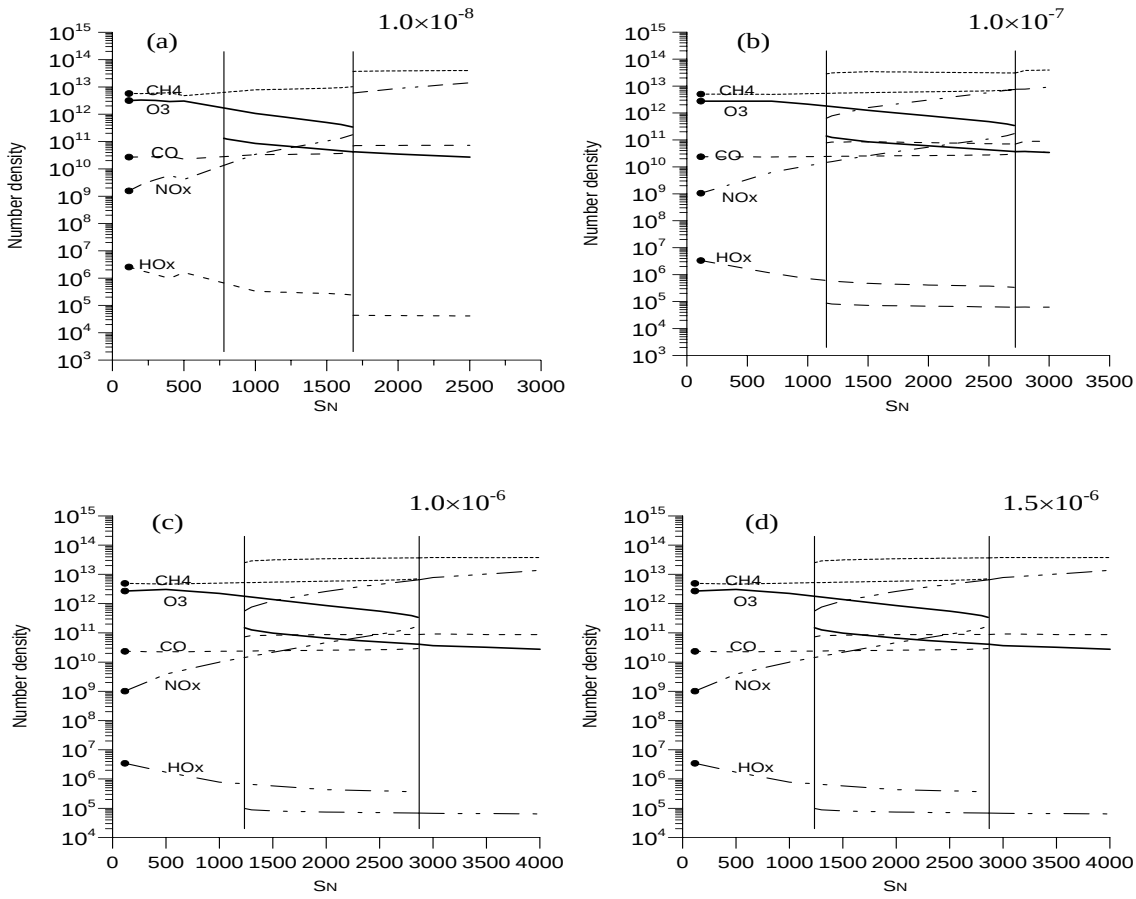

Fig. 2. Same as Fig. 1, but for S_{CH_4} chosen as 1800 cm^{-3} s^{-1}.

like those in Fig. 1 are also found, and the topological structure of this system has no obvious change compared to that in test-I, which always keeps the "fold" catastrophe in the space $P\,(S_N, A)$. However, for each multi-equilibrium solution. which are located at [760, 1685], [1150, 2730], [1235, 2870], [1235, 2870] for A=1, 10, 100, 150 (in Figs. 2a–2d), respectively, it shows that the corresponding widths of their the multi-equilibrium solutions are much more increased than in test-I for all the cases with the increase of the CH_4 source. The increase in the widths of the multi-equilibrium solutions means that, if the catastrophic transition has occurred, the parameter S_N requires a greater reduction in order to return to the original equilibrium branch. Furthermore, the location leading to catastrophic transition points of S_N is far away from the current value (S_N=115) with the increase of A.

4. Response for when both S_{Cl} and A change

In the following section, we discuss the behaviors of the system in another 2-D parameter space $P\,(S_{Cl},\, A)$. S_N remains at the current value of 115, and the other parameters are taken as the current values given in Tables 1, 2, 3 unless otherwise specified.

4.1 *Result of test-I*

Figure 3 gives the solutions of the system when $13 \leqslant S_{Cl} \leqslant 300$ for $S_{CH_4} = 1000$ cm^{-3} s^{-1}, and A is fixed at 1,10,100 and 150. When $A = 1$ (Fig. 3a), in the parameter of the S_{Cl} domain, no multi-equilibrium solutions like in Fig. 1 or Fig. 2 are found. This is due to the fact that when S_{Cl} is nearly less than 170, the number density of O_3 is almost unchanged depending on the increase of S_{Cl}, whereas it is sensitive to S_{Cl} in the period when S_{Cl} is greater than 170. When $A = 10$ (Fig. 3b), the sensitive value is near 110 which is earlier than that in $A = 1$. But with the increase of A, as $A = 100$ (Fig. 3c), the structure of this photochemical system changes and multi-equilibrium solutions occur, and the domain of the multi-equilibrium solution is over [67, 69]. Furthermore, as $A = 150$ (Fig. 3d), its

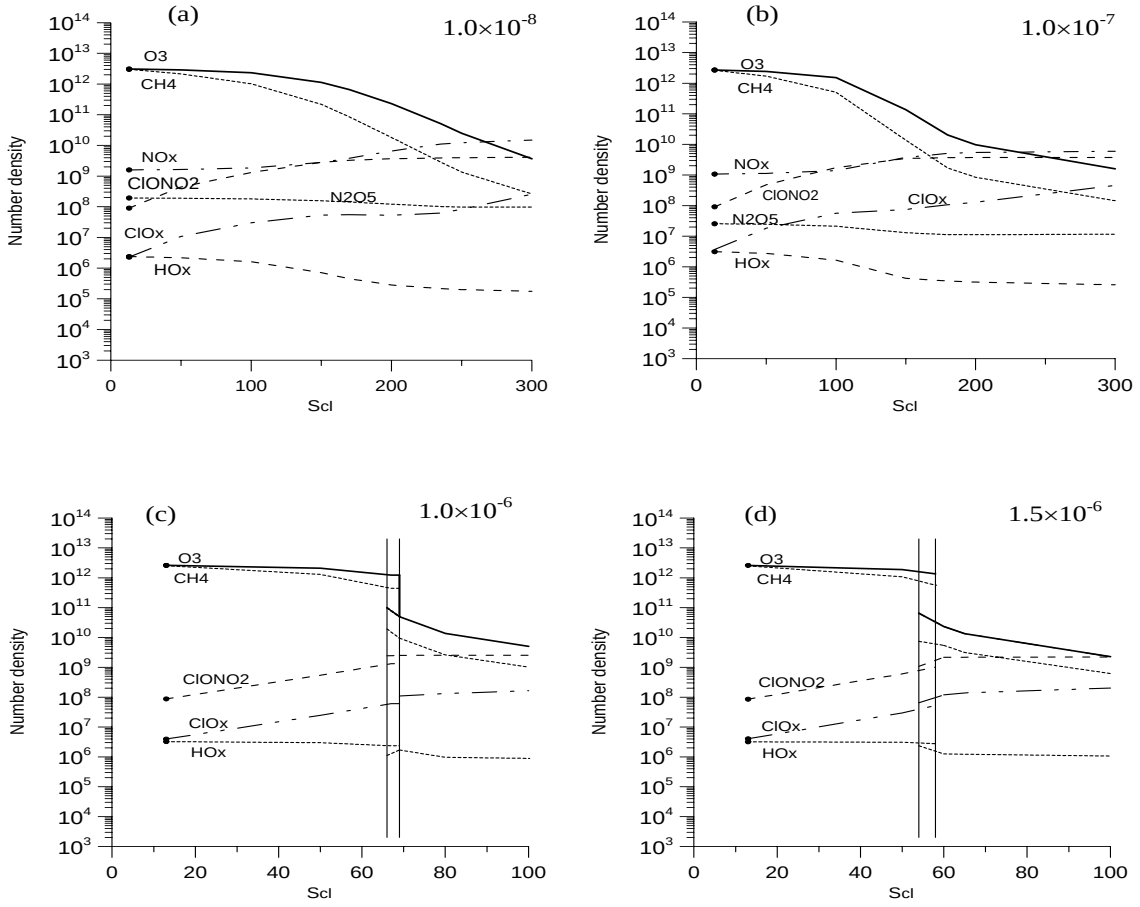

Fig. 3. Dependence of the states of the heterogeneous system on the aerosol surface area density A and the reactive chlorine resource S_{Cl} for $S_{\mathrm{CH_4}}$ chosen as $1000\,\mathrm{cm^{-3}\,s^{-1}}$.

corresponding multi-equilibrium solution is located at [54, 58], and this location leads to the catastrophe transition being close to its current value $S_{\mathrm{Cl}} = 13$. This result indicates that an increase of about 4 times of the current value of S_{Cl} could lead to the catastrophe transition. At this time, the equilibrium concentration of ozone is reduced by about 100 times in magnitude.

4.2 *Result of test-II*

Figure 4 gives the solutions of this system when $13 \leqslant S_{\mathrm{Cl}} \leqslant 300$, and A is fixed at 1, 10, 100 and 150 for $\mathrm{S_{CH_4}}$ being $1800\,\mathrm{cm^{-3}\,s^{-1}}$. From Fig. 4a and Fig. 4b, we see that the solutions of the system have a similar structure to that shown in Figs. 3a and 3b. However, the sensitive value of S_{Cl} is near 260 (in Fig. 4a) and 180 (in Fig. 4b) which both depart from the current value in test-I.

With the increase of A, as in the case of $A = 100$ (in Fig. 4c), some dramatic changes occur in the ozone concentrations; constitutions of the solution are as follows (here is a basic sketch of ozone number density dependence on A and S_{Cl}): When S_{Cl} increases to near 150 from the current value 13, a supercritical Hopf bifurcation takes place. The original equilibrium solution loses stability and a new stable periodic solution appears. When S_{Cl} increases to near 170, an abrupt change occurs, and the state of the ozone system jumps to another equilibrium state with the ozone concentration being reduced by about 10 times in magnitude; when S_{Cl} decreases to 135 from 250, it changes to a periodic solution from an equilibrium one through Hopf bifurcation; with the decrease of S_{Cl} to near 116, an abrupt transition happens and it jumps to a higher equilibrium solution. When $A = 150$ (in Fig. 4d), it is similar to Fig. 4c, and only the sensitive region changes with S_{Cl}. When S_{Cl} increases to 105 from the current state, the state of this photochemical system turns into a periodic solution from an equilibrium one via Hopf bifurcation. When S_{Cl} increases to 150, the abrupt

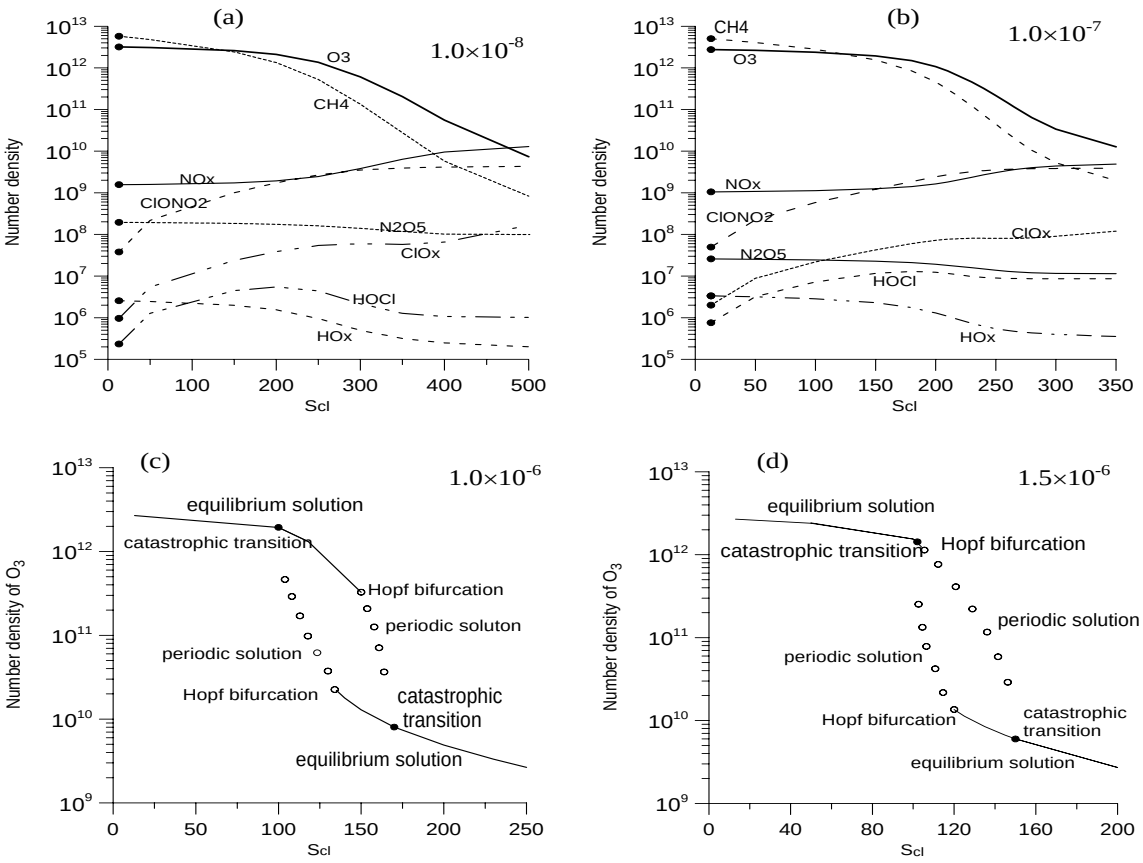

Fig. 4. Same as Fig. 3, but for S_{CH_4} chosen as 1800 cm^{-3} s^{-1}.

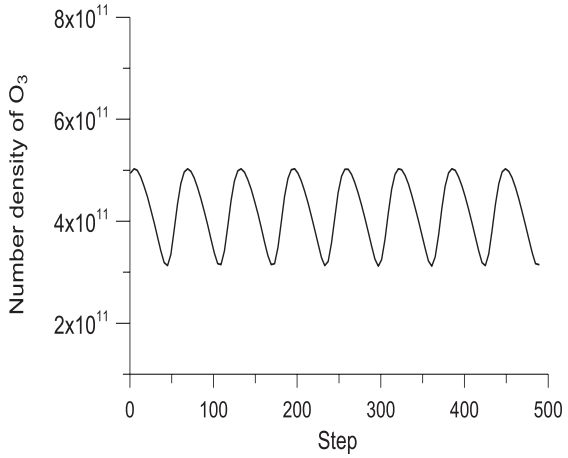

Fig. 5. Periodic solution of ozone density dependence on time obtained for S_{Cl}=133 cm^{-3} s^{-1} and S_N=115 cm^{-3} s^{-1} when $A = 100 \times 10^{-8}$ cm^{-1}, $S_{CH_4} = 1800$ cm^{-3} s^{-1}.

change takes place near this point, and the state of the system shifts to a new lower equilibrium state; when S_{Cl} decreases to 118 from 200, it changes to a periodic solution from an equilibrium one via Hopf bifurcation. With the continued decrease of S_{Cl} to near 103, an abrupt transition occurs and it jumps to a higher equilibrium solution. A periodic solution of ozone density dependence on time for S_{Cl}=133 cm^{-3} s^{-1} and S_N=115 cm^{-3} s^{-1} when $A = 100 \times 10^{-8}$ cm^{-1} is provided in Fig. 5.

5. Discussion and conclusions

This paper continues the investigation (Yang and Brasseur, 2004) of non-linear behaviors of the lower stratospheric photochemical system. Moreover, this study is in view of the fact that natural emissions of ClO_x and NO_x are rather uncertain and that anthropogenic emissions have rapidly increased in recent years (Crutzen and Birks, 1982; WMO, 1995; Fraser and Prather, 1999). In addition, CH_4 is the most abundant hydrocarbon in the atmosphere and is useful as a tracer of atmospheric circulation; its concentrations have also increased in the atmosphere (WMO, 1995).

Under these considerations, we use a zero-dimensional box photochemical model incorporating the more important chemical and photochemical processes, especially the main heterogeneous processes, in the mid-latitude lower stratosphere at the time of the spring equinox and expect to theoretically analyze

the behaviors of the lower stratospheric photochemical system in response to enhanced atmospheric abundances of sulfate aerosol and reactive nitrogen and chlorine as well as increasing CH_4 sources.

The results given in sections 3 and 4 show that the present modeled photochemical system can present several different solutions, for instance, periodic states and multi-equilibrium states under some certain parameter domains, through chlorine chemistry and nitrogen chemistry together with sulfate aerosol as well as the increasing magnitude of CH_4 sources.

These qualitative results reveal that although locations leading to catastrophic transition points are far away from the current value of reactive nitrogen and chlorine, they might have the possibility to occur under some extreme abnormities.

The results of our paper contribute to the understanding of the possible future evolution of the atmospheric ozone in the lower mid-latitude stratosphere under the conditions of the increasing external forcing strength by reactive nitrogen and chlorine with different magnitudes of CH_4 sources. Actually, the existence of the nonlinear effects in the box models employed in these studies is conditioned by the presence of influxes and sinks of chemical constituents, which are due to transport processes, however, an analysis of the photochemistry within the frameworks of the box models suggests that the transport processes involved should be parameterized in the simplest manner. In addition, photolytic processes in this box model do not change with time, which is due to the fact that this box model is applied in a fixed situation and the temperature circumstances are assumed to be stable. However in the real atmosphere, these processes are sensitive to the temperature, but such feedback in this model is ignored, and this will be investigated in our future studies.

Acknowledgments. This work was supported by the National Natural Science Foundation of China under grant Nos. 90411009 and 40505018.

REFERENCES

Bojkov, R. D., 1995: The international ozone assessment, 1994, WMO/UNEP, **44**, 42–50.

Crutzen, P. J., and J. W. Birks, 1982: The atmosphere after a nuclear war: Twilight at noon. *J. Ambio*, **23**, 114–125.

Fraser, P. J., and M. J. Prather, 1999: Uncertain road to ozone recovery. *Nature*, **398**, 663–664.

Fried, A., B. E. Henry, J. G. Calvert, and M. Mozurkewich, 1994: The reaction probability of with sulfuric acid aerosols at stratospheric temperatures and compositions. *J. Geophys. Res.*, **99**, 3517–3532.

Gear, C. W., 1969: The automatic integration of stiff ordinary differential equations. *Proc IFIP Congress*, North Holland, 187–193.

Granier, C., and G. Brasseur, 1992: Impact of heterogeneous chemistry on model predictions of ozone changes. *J. Geophys. Res.*, **97**, 18015–18033.

Hofmann, D. J., and S. Solomon, 1989: Ozone destruction through heterogeneous chemistry following the eruption of El Chichon. *J. Geophys. Res.*, **94**, 5029–5041.

Kasting, J. F., and T. P. Ackerman, 1985: High atmospheric NOx levels and multiple photochemical steady state. *Journal of Atmospheric Chemistry*, **3**, 321–340.

Konovalov, I. B., M. F. Alexander, and A. Y. Mukhina, 1999: Toward understanding of the nonlinear nature of atmospheric photochemistry: Multiple equilibrium states in the high-latitude lower stratosphereric photochemical system. *J. Geophys. Res.*, **104**, 3669–3689.

McCormick, M. P., and R. E. Veiga, 1992: SAGE II measurement of early Pinatubo aerosols. *Geophys. Res. Lett.*, **19**, 155–158.

Mozurkewich, M., and J. G. Calvert, 1988: Reaction probabilities of N_2O_5 on aqueous aerosols. *J. Geophys. Res.*, **93**, 15889–15896.

Prather, M. J., M. B. McElroy, S. C. Wofsy, and J. A. Logan, 1979: Stratospheric Chemistry: Multiple solutions. *Geophys. Res. Lett.*, **6**, 163–164.

Prather, M. J., 1992: Catastrophic loss of stratospheric ozone in dense volcanic clouds. *J. Geophys. Res.*, **97**, 10187–10191.

Rodriguez, J. M., K. W. K. Malcolm, and D. S. Nien, 1991: Role of heterogeneous conversion of N_2O_5 on sulfuric aerosols in global ozone losses. *Nature*, **352**, 134–137.

Stewart, R. W., 1993: Multiple steady states in atmosphereric chemistry. *J. Geophys. Res.*, **98**(20), 20601–20612.

Stewart, R. W., 1995: Dynamics of the low to high NOx transition in a simplified tropospheric photochemical model. *J. Geophys. Res.*, **100**, 8929–8943.

Tie, X. X., G. Brasseur, B. Briegleb, and C. Granier, 1994: Two dimensional simulation of Pinatubo aerosol and its effect on stratospheric ozone. *J. Geophys. Res.*, **99**, 20545–20562.

White, W. H., and D. Dietz, 1984: Does the photochemistry of the troposphere admit more than steady state? *Nature*, **309**, 242–244.

WMO, 1992: Scientific assessment of ozone depletion: 1991. Report No.29, Geneva.

WMO, 1995: Scientific assessment of ozone depletion: 1994. Report No.37, Geneva.

Worsnop D. M., and Coauthors, 1988: Mass accommodation coefficient measurements for HNO_3, HCl and N_2O_5 on water, ice and aqueous sulfuric acid droplet surfaces. Polar ozone workshop, National Aeronautics and Space Administration, Snowmass, Colo., May 1988.

Yang, P., and G. Brasseur, 1994: Dynamics of the oxygen-hydrogen system in the mesosphere, I, Photochemical equilibrium and catastrophe. *J. Geophys. Res.*, **99**(20), 20955–20966.

Yang, P., and G. Brasseur, 2001: The nonlinear response of stratospheric ozone to NO_x and ClO_x perturbations. *Geophys. Res. Lett.*, **28**, 717–720.

Yang, P., and G. Brasseur, 2004: Mathematical analysis of the stratospheric photochemical system. *J. Geophys. Res.*, **109**, D15308, doi:10.1029/2003JD004028.